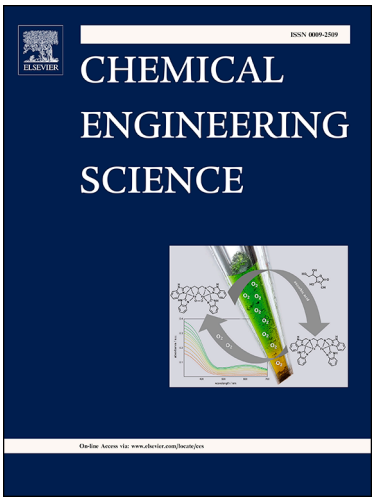

Integrated ionic liquid and process design involving azeotropic separation processes

Yuqiu Chen, Rafiqul Gani, Georgios M. Kontogeorgis, John M. Woodley

PII: S0009-2509(19)30369-0
DOI: https://doi.org/10.1016/j.ces.2019.04.005
Reference: CES 14916

To appear in: *Chemical Engineering Science*

Received Date: 31 October 2018
Revised Date: 28 March 2019
Accepted Date: 3 April 2019

Please cite this article as: Y. Chen, R. Gani, G.M. Kontogeorgis, J.M. Woodley, Integrated ionic liquid and process design involving azeotropic separation processes, *Chemical Engineering Science* (2019), doi: https://doi.org/10.1016/j.ces.2019.04.005

Integrated ionic liquid and process design involving azeotropic separation processes

Yuqiu Chen [a], Rafiqul Gani [b,c], Georgios M. Kontogeorgis [a], John M. Woodley [a,*]

[a] *Department of Chemical and Biochemical Engineering, Technical University of Denmark*

DK-2800 Lyngby, Denmark

[b] *PSE for SPEED, Skyttemosen 6, DK-3450 Allerod, Denmark*

[c] *State Key Laboratory of Industrial Control Technology, College of Control Science and Engineering, Zhejiang University, Hangzhou 310027, China*

[*]Corresponding author. Tel.: +45 45252885. *E-mail address:* jw@kt.dtu.dk (J.M. Woodley)

Abstract

In process industries, separation techniques need to be employed to match product quality and purity specifications. Most vapour-liquid based separation techniques involving the separation of close-boiling or azeotropic as well as gaseous mixtures are energy intensive. Downstream separations from bioreactors are, on the other hand, difficult because of relatively small amounts of products in large amounts of reactants and carriers such as water. With growing energy and environmental challenges, novel, sustainable and innovative separation techniques are receiving increasing attention. Because of their non-volatility and other tuneable properties, ionic liquids (ILs) based separation techniques are promising alternatives. In this work, a systematic method that combines group contribution (GC)-based property prediction and IL-based separation process design is presented. That is, the optimal IL molecular structure and the corresponding optimal flowsheet configuration for a specific IL-based separation process are simultaneously identified. Case studies involving the separation of azeotropic mixtures such as ethanol-water and acetone-methanol are presented to highlight the application of the method for synthesis-design of the IL-based separation technology.

Keywords: Ionic liquids, CAMD, Azeotrope separation, UNIFAC-IL model, Group contribution method

1. Introduction

The pressing challenges related to energy, water, food and environment emphasize the need for new sustainable and innovative process designs. Consequently, the integration of new technologies into existing process designs is an attractive option for the industry. As a common processing step in chemical and related process industries, separation processes accounts for 10-15% of the world's energy consumption (Sholl and Lively, 2016). Its efficiency could drive the future development of the industry in terms of energy consumption and capital investment. Therefore, intensified separation alternatives are attractive, especially for those involved with energy intensive separation processes (Lutze et al., 2010, Babi et al., 2015). In bio-processes, the downstream separations lead to major costs and wastes in manufacturing due to the recovery of relatively small amounts of products from dilute aqueous solutions (Woodley et al., 2008, Woodley, 2017). Separation of close-boiling, azeotropic mixtures, and CO_2 removal are examples of high energy consuming processes (Chen et al., 2018, Vooradi et al., 2017). It is advantageous to investigate new technologies that allow energy efficient operation for such energy intensive or difficult separation processes.

Among many potential separation technologies, the use of ionic liquids (ILs) as solvents is being considered because of their non-volatility and therefore low energy consuming solvent recovery operations (Seiler et al., 2004, Lei et al., 2014b). Additionally, unlike most conventional organic solvents that may also be classified as volatile organic chemicals (VOCs), which would escape into the atmosphere, ILs exhibit attractive features such as almost negligible vapor pressure, wide liquidity range, high thermal and chemical stability (Rogers and Seddon, 2003). Moreover, ILs have been found to provide good solubility and selectivity for a wide range of both organic and inorganic chemicals (Welton, 1999), which are important for separation processes. Therefore, ILs could be considered as attractive alternatives for the replacement of VOCs in many separation processes. To date, industrial application of ILs is still limited mainly because of their high cost and operational constraints (e.g. high viscosity) (Shamsuri, 2011). Moreover, the understanding of their toxicity and environmental impact is not complete (Petkovic et al., 2011). However, these limitations can be addressed through appropriate selection of IL and synthesis-design of the separation process.

Research regarding the use of ILs as designer solvents in separation processes has been in focus, mainly for acid gas removal, IL-based extraction and extractive distillation. To identify the potential of ILs for acid gas removal from gas streams, (Mortazavi‐Manesh et al., 2013) developed semi-empirical models for the solubility of H_2S, CH_4, and C_2H_6, in which the activity coefficients of solutes in ILs is predicted using a conductor-like screening model for realistic solvation (COSMO-RS), while, the gas fugacity coefficients are calculated using a cubic EOS. Chong et al. (2015) proposed an approach based on the visualization of higher dimensional problems into two or three dimensions for design of ILs for CO_2 capture. Chong et al. (2016) subsequently introduced disjunctive programming to identify optimal operating conditions of the carbon capture process while also solving the IL design problem. Zhao et al. (2017) used COSMO-RS to establish a database of predicted Henry's law constants for twelve gases in a large number of ILs at 313.15 K and, using this database, proposed a systematic screening method of ILs for separation of gases by absorption. Most recently, a systematic study combining an extended UNIFAC-IL model for phase equilibrium together with other group contribution (GC) models for prediction of viscosity and melting point of ILs has been proposed by Song et al. (2018), where optimal ILs for the extractive desulfurization system (EDS) of fuel oils are identified by formulating and solving a mixed-integer non-linear programming (MINLP) problem.

For IL-based extraction and extractive distillation, 1-butyl-1-methylpyrrolidinium bis (trifluoromethylsulfonyl) imide $[C_4mPyr][Tf_2N]$ has been proposed and tested as a solvent for separation of paraffins from aromatics by Pereiro and Rodríguez (2010). The results show that IL-based extraction is a promising alternative to well-known organic solvent (sulfolane) based extraction in terms of energy requirements. Roughton et al. (2012) proposed an UNIFAC model based method for simultaneous design of ILs and the process for separation of azeotropes. Fang et al. (2016) presented a molecular design method using the COSMO-SAC model to select ILs for extractive distillation. A study combining the UNIFAC-IL model and other GC-based property models for IL design and process simulation has been reported by Chao et al. (2017) to identify promising ILs for the separation of n-hexane and methyl cyclopentane by extractive distillation. A common deficiency with all these methods is that the designed ILs have been selected based on their implicit separation task related properties and IL performance checked through off-line process simulation. Therefore, the optimal energy consumption, equipment design or the capital cost have not been determined.

The solvent has significant impact on the overall performance and economics of separation processes and is usually selected on the basis of experience, heuristic rules, or a few

exploratory experiments. Generally, a specific IL comprises an anion and a cation, in which the side position(s) of the cation can be attached to various substituents. This results in more than several thousand possible ILs (Holbrey and Seddon, 1999). Finding optimal ILs for specific separation tasks by the usual trial-and-error approach can, therefore, be time consuming and expensive due to the numerous ILs that may be considered as potential solvents. To overcome the limitations of such selection methods, computer-aided molecular design (CAMD), a systematic approach that integrates property predictive models and optimization algorithms to reverse engineer molecular structures with unique properties (Gani et al., 1991, Harper et al., 1999), is ideally suited. In this way, tailor-made ILs can be generated by adjusting the cations, anions, and substituents (Plechkova and Seddon, 2008). Thus, the "generate and test" approach of generating candidate ILs by tailoring their properties and testing them on the desired separation task is suitable for the design of ILs, as well as for design-verification of their ability to perform specific separation tasks.

Generally, the properties of ILs directly or indirectly impact the performance of the process in which the IL is employed as solvent. However, the classical two-stage design method (molecular design followed by process design) cannot fully represent the strong interdependencies between solvent properties and process performance. Thus, some trade-offs are necessary between tailor-made solvent properties in the design of whole chemical processes. For example, in the context of an extraction process, the selected solvent must offer both high capacity, selectivity and easy recovery for the species to be extracted. Alongside, properties such as viscosity and surface tension should also be considered because of their impact on the process operation and the size of processing units. Based on the reduced models of processing units (e.g. absorber, flash drum), integrated design method was used by Pereira et al., (2011) and Burger et al., (2015) on CO_2 capture process with organic solvents. Similarly, Zhou et al., (2015) optimized molecular structure (organic solvent) and process operations on the Diels-Alder reaction by using an integrated design method. For using ILs as solvents, Valencia-Marquez et al., (2011) integrated IL and separation process design for ethanol-water mixture with promising results. However, in their work, the cost of the IL regeneration step is not included and only specific cation (imidazolium)-anion configurations are considered, which resulting in a limited design space of both IL structure and process configurations. In this work, an integrated approach, where IL molecular design together with separation process synthesis-design is solved simultaneously, is presented. All groups (i.e. cations, anion, and substituents) are considered for IL molecular generation together with the cost of IL regeneration step. The application of the integrated IL and process synthesis-design method is highlighted through two case studies involving the separation of azeotropic mixtures.

2. Methodology

2.1. Framework

A framework for integrated IL and process design has been developed, as highlighted in Figure 1. It has five main sections: a) Property model library (GC-based property models, UNIFAC-IL model); b) IL structure (IL-groups set, IL structural parameters, CAILD); c) Process and cost models; d) Integrated IL and process design (MINLP problem formulation and solution); e) Solution and validation (use an appropriate solver and validate the solution through process analysis or experiments (if available).

The work-flow employed by the methodology is as follows: First, retrieve the necessary GC-based property (e.g. density, viscosity, surface tension) models, the regressed UNIFAC-IL

model parameters, and the collected group sets (i.e. cations, anions, substituents) from the model library contained in the IL database for the design of IL. Second, formulate the CAILD problem. Third, add the UNIFAC-IL model equations, the GC-based property models, the process and cost models, to formulate the integrated IL and process design problem as a MINLP model. Fourth, solve the MINLP problem with an appropriate solver to obtain, for example, the identified IL, process operating conditions, equipment sizing parameters and associated costs. Fifth, verify the optimal solution through analysis and/or experiment.

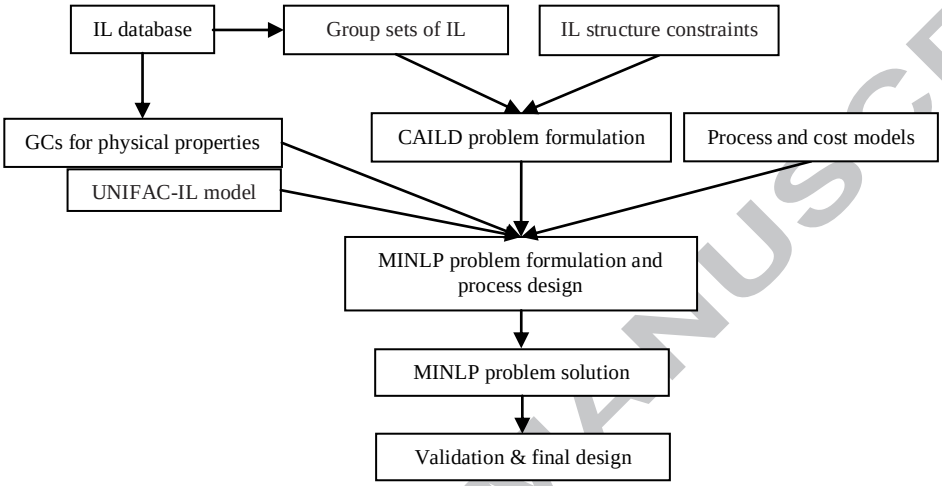

Figure 1: Framework of the integrated ionic liquid and process design

2.2. GC-based property models

Properties of ILs are essential for the design of products and processes containing ILs. For example, to avoid solidification of the solvent, the melting point of the selected IL must be at least 5 K less than the temperature (T_p) at every point in the whole process. To date, only a small number of ILs have been reported and the available experimental data on their properties is still scarce and limited to the well-studied ILs. Moreover, experimental data from different literature sources are sometimes contradictory. With consideration of the potential ILs and their very large number, to measure the properties for all conceivable ILs is impractical. Therefore, empirical or theoretical methods are promising and alternative ways to obtain the required information of their properties.

Currently, several methods have been presented for the estimation of IL properties (Jacquemin et al., 2008a, Jacquemin et al., 2008b, Lazzús, 2009, Gardas and Coutinho, 2009, Huang et al., 2013, Mousazadeh and Faramarzi, 2011). Among them, GC-based methods are popular since these methods can be used easily and they are also the basis of using the CAMD method, which in a systematic manner can identify optimal ILs containing the desired properties for specific applications confidently and rapidly, as mentioned above.

In our previous work (Chen et al., 2019), a comprehensive database has been established by collecting numerous experimental data of IL properties from different literature sources and also by apriori combinations of new ILs. The database includes 4960 ILs covering 7 cations and 16 anions, out of which around 300 have been synthesized.

As shown in Eq.1 and Eq.2, two types of property model, i.e. GC-based pure component property (θ_i) models and GC-based mixture property (θ_{mix}) models using the ideal mixing rule, are considered for the properties (e.g. density, heat capacity) involved in this work.

$$\theta_i = \sum_{k=1}^{N} n_{k,i}\delta_k \quad (1)$$

$$\theta_{mix} = \sum_{i=1}^{M} x_i\theta_i \quad (2)$$

where N is the total number of groups representing the IL. δ_k represents the property contribution of group k for pure component property θ_i and $n_{k,i}$ denotes the number of group k in component i. M and x_i are the total number of components and the mole fraction of component i in mixture, respectively.

The IL property model library includes GC-based models for density (Eq.3 and 4), heat capacity (Eq.5 and 6), viscosity (Eq.7 and 8), surface tension (Eq.9 and 10) and melting point (Eq.11). Note that these physical properties of ILs directly or indirectly impact the process performance where the IL is employed as the separating agent and all of these property models are taken from our previous work (Chen et al., 2019).

$$\rho = A_\rho + B_\rho \cdot T + C_\rho \cdot P \quad (3)$$

where ρ (kg.m^{-3}) is density, T (K) is temperature and P (bar) is pressure. A_ρ, B_ρ and C_ρ are parameters that can be calculated from the GC-based method by Eq.4

$$A_\rho = \sum_{i=1}^{k} n_i a_{i,\rho} \quad B_\rho = \sum_{i=1}^{k} n_i b_{i,\rho} \quad C_\rho = \sum_{i=1}^{k} n_i c_{i,\rho} \quad (4)$$

where k is the total number of different groups appeared in the molecule, n_i denotes the number of groups of type i and the group contributions are represented by $a_{i,\rho}$, $b_{i,\rho}$ and $c_{i,\rho}$.

$$C_{pL} = R\left(A_{C_{pL}} + B_{C_{pL}}\left(\frac{T}{100}\right) + D_{C_{pL}}\left(\frac{T}{100}\right)^2\right) \quad (5)$$

where C_{pL} (J.mol^{-1}.K^{-1}) is the heat capacity and T (K) represents the absolute temperature, and R represents the gas constant (8.3145 J.mol^{-1}.K^{-1}). Parameters $A_{C_{pL}}$, $B_{C_{pL}}$ and $D_{C_{pL}}$ can be obtained from group contributions, as shown in Eq.6.

$$A_{C_{pL}} = \sum_{i=1}^{k} n_i a_{i,C_{pL}} \quad B_{C_{pL}} = \sum_{i=1}^{k} n_i b_{i,C_{pL}} \quad D_{C_{pL}} = \sum_{i=1}^{k} n_i c_{i,C_{pL}} \quad (6)$$

where k is the total number of different groups in the IL molecule and n_i is the number of groups of type i; $a_{i,C_{pL}}$, $b_{i,C_{pL}}$ and $d_{i,C_{pL}}$ are the group contributions

$$\ln\frac{\eta}{R_{0\eta}} = A_\eta + B_\eta\frac{100}{T} + D_\eta\left(\frac{100}{T}\right)^2 \quad (7)$$

where η (Pa.s) is viscosity and T (K) is temperature. $R_{0\eta}$ is an adjustable parameter. A_η, B_η and C_η can be obtained by a GC-based method according to

$$A_\eta = \sum_{i=1}^{k} n_i a_{i,\eta} \quad B_\eta = \sum_{i=1}^{k} n_i b_{i,\eta} \quad D_\eta = \sum_{i=1}^{k} n_i d_{i,\eta} \quad (8)$$

where k represents the total number of different groups in the molecule, n_i denotes the number of groups of type i and the group contributions are described as $a_{i,\eta}$, $b_{i,\eta}$ and $d_{i,\eta}$

$$\ln\sigma = A_\sigma + B_\sigma\left(\frac{T}{100}\right) + D_\sigma\left(\frac{T}{100}\right)^2 \quad (9)$$

where σ (N.m^{-1}) is surface tension and T (K) is temperature. A_η, B_η and C_η are parameters that can be achieved by GC-based method, as shown in Eq.10

$$A_\sigma = \sum_{i=1}^{k} n_i a_{i,\sigma} \quad B_\sigma = \sum_{i=1}^{k} n_i b_{i,\sigma} \quad D_\sigma = \sum_{i=1}^{k} n_i d_{i,\sigma} \quad (10)$$

where k is the total number of different groups in the molecule and n_i is the number of groups of type i; $a_{i,\sigma}$, $b_{i,\sigma}$ and $d_{i,\sigma}$ represent the group contributions.

$$T_m = \sum_{c=1}^{k_c} n_c t_c + \sum_{a=1}^{k_a} n_a t_a + \sum_{g=1}^{k_g} n_g t_g \quad 11$$

where T_m (K) is the melting point. Parameters t_c, t_a and t_g are the group contributions of cations, anions and substituents for the melting point while n_c, n_a and n_g represent the number of cations, anions and substituents in the IL molecule, respectively.

2.3. UNIFAC-IL model

The predictions of solubility and phase equilibria are essential for the design of ILs as solvents in separation processes. Several predictive thermodynamic methods have been proposed for IL containing systems, among which apriori methods such as COSMO-RS (Klamt, 1995, Klamt et al., 1998, Klamt and Eckert, 2000) and COSMO-SAC (Lin and Sandler, 2002, Lin et al., 2004) that directly convert the atom information of compounds into thermodynamic data have been widely studied. These methods are very efficient for screening ILs since only the molecular information is required (Diedenhofen et al., 2003, Kato and Gmehling, 2005, Lei et al., 2007). However, sometimes the calculated thermodynamic properties of solutes in ILs using COSMO methods are not consistent with experimental data (Palomar et al., 2011). Thus, work for improving the prediction accuracy of these methods is needed. Activity coefficient models like UNIQUAC and NRTL that require interaction parameters fitted from experimental data have been introduced to the IL containing systems (Simoni et al., 2008, Santiago et al., 2009). These models are able to provide prediction results with high accuracy. In addition, equations of state such as GCLF and PC-SAFT have also been extended to predict the thermodynamic behavior of IL-involved systems, and reliable prediction can be achieved using these models (Lei et al., 2012b, Dai et al., 2013).

By representing molecules with functional groups as in GC-based property prediction in section 2.2, the UNIFAC model can be used to predict activity coefficients for the compounds in solution (Gmehling and Rasmussen, 1977, Gmehling et al., 1982, Tiegs et al., 1987, Wittig et al., 2003). This GC-based approach has been extended to IL containing systems (Kato and Gmehling, 2005, Lei et al., 2009). To date, works regarding a UNIFAC-IL model have been presented and the interaction parameters involving well-studied IL groups have been regressed by Lei et al. (2009), Lei et al. (2012a), Lei et al. (2014a), Roughton et al. (2012), Hector and Gmehling (2014). Due to the advantages of using UNIFAC as a thermodynamic model in the IL containing systems mentioned above, UNIFAC-IL has been selected as the thermodynamic method in the methodology proposed in this work. The UNIFAC-IL model equations are given in Appendix A.

Using the same functional groups to calculate the target pure component and mixture properties in Eqs. 1-2 as well as the UNIFAC-IL (extended UNIFAC model for ILs), an integrated computer-aided IL design method can be easily developed, to be called, CAILD.

To estimate the liquid phase activity coefficients of ILs in solution with the UNIFAC-IL model, appropriate representation of the ILs is required. Three alternatives have been highlighted by Lei et al. (2012a), Lei et al. (2013):

(1) The IL is divided into one cation-based group and one anion group (see Figure 2.I);

(2) The IL is divided into several groups with the skeletons of the cation and the anion treated as a whole (see Figure 2.II);

(3) The IL is divided into several groups with the cation skeleton treated as a separate group (see Figure 2.III).

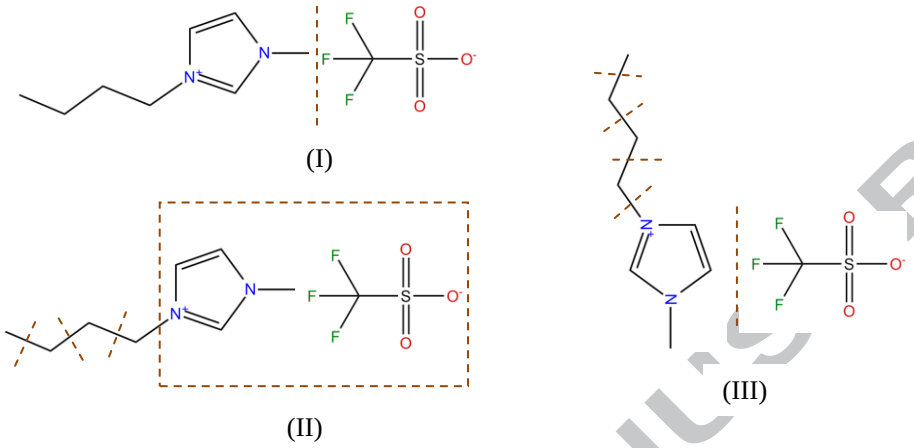

Figure 2. Three different decomposition approaches of IL for UNIFAC functional groups: Exemplified for1-butyl-3-methylimidazolium trifluoroacetate ($[C_4mIm]^+[CF_3SO_3]^-$).

The third approach is employed in this work as the design space and the flexibility of CAILD is significantly enlarged when IL is divided into cation, anion, and substituents separately (Song et al., 2018), and the developed GC property models in section 2.1 also represent ILs in this manner.

2.4. CAILD Method

The integrated IL and process design problem is formulated as a mixed-integer non-linear programming (MINLP) optimization problem given by Eqs.12-17 In this work, the MINLP problem formulation from (Burger et al., 2015) has been adopted.

$$max/min_{z,y}\, f(z,y) \tag{12}$$

$$s.t. \quad g_p(z,y) = 0 \tag{13}$$

$$g_t(z,y) \leq 0 \tag{14}$$

$$g_m(y) \leq 0 \tag{15}$$

$$z \in R^w \tag{16}$$

$$y \in U^q \tag{17}$$

where the m -dimensional vector z represents continuous variables involving mixture composition, physical properties, operating conditions, equipment sizes and process variables; the q -dimensional vector of integer and binary variables y denoting the molecular (IL) structure; f is the objective function, typically an economic performance metric (e.g. profit, capital investment) , to be maximized or minimized subject to a set of constraints. g_p and g_t are sets of equality constraints and inequality constraints representing the process model and the thermodynamic model, respectively. Molecular (IL) structure feasibility and valency rules are represented by constraints g_m.

Gm constraints (molecular structure of ILs)

The design of ILs requires a systematic combination of various functional cations, anions and substituents based on certain structure constraints to generate feasible ILs of desired properties. A detailed set of constraints, shown in Eqs.18–24, is employed to ensure the feasibility and complexity of designed ILs (Karunanithi and Mehrkesh, 2013).

$$\sum_{i\epsilon C} c_i = 1 \quad (18)$$

$$\sum_{j\epsilon A} a_j = 1 \quad (19)$$

$$\sum_{l=1}^{N} x_l - \sum_{i\epsilon C} c_i v_i = 0 \quad (20)$$

$$\sum_{i\epsilon C}(2 - v_i)c_i + \sum_{l=1}^{N}\sum_{k\epsilon S}(2 - v_{kl})x_l\, n_{kl} = 2 \quad (21)$$

$$\sum_{k\epsilon S}(2 - v_{kl})x_l n_{kl} = 1 \quad (22)$$

$$n_S^L \le \sum_{l=1}^{N}\sum_{k\epsilon S} x_l n_{kl} \le n_S^U \quad (23)$$

$$n_{Sl}^L \le \sum_{k\epsilon S} x_l n_{kl} \le n_{Sl}^U \quad (24)$$

where C is the set of cations (e.g. imidazolium, pyridinium) and A is the set of anions (e.g. tetrafluoroborate, hexafluorophosphate); the vector c_i and a_j are binary variables representing the occurrence of the cations and the anions, respectively. For example, the value of the binary variable is equal to 1 when a group is included in the IL molecular, otherwise its value is 0. The occurrence of the side chains, l, are represented by the vector x_l of binary variables, while the number of substituents (e.g. methyl, methylene) of type k in the side chain l is described by the vector n_{kl} of integer variables. v_i, v_{kl} are vectors denoting group valences of the cations and substituents, respectively. S is the set of substituents for the cation side chains. Only one cation and one anion is available in each IL candidate (Eqs.18 and 19). The octet rule (Eq.20) ensures the consistency between the number of side chains and the available free valence of the cation base. In the chemical structure of IL, side chains are only attached to the cation; Eqs.33 and 34 are utilized to ensure that any two adjacent groups are not linked by more than one covalent bond. In Eqs.20, 21 and 23, N represents the total number of available side chains. Considering the size and complexity of typical IL molecules, minimum and maximum numbers of substituents n_S^L, n_{Sl}^L and n_S^U, n_{Sl}^U are specified for the cation and each side chain l, respectively (Eqs.23 and 24).

3. Process and cost models

3.1. Process models

Although it is an energy intensive process, the separation of azeotropic mixtures is widely found in the chemical and petrochemical industries. In downstream separations of pharmaceuticals and in biochemical processes, azeotropes are also encountered and increase the difficulties in these industrial sectors (Barton, 2000, Simoni et al., 2010). Extractive distillation is an attractive technique for separating azeotropic mixtures since the selected entrainer can break the azeotrope by interacting with the components (Benedict and Rubin, 1945). The selection of the entrainer is a common concern in extractive distillation. Unlike VOCs that can escape into the atmosphere because of their high volatility, ILs possess attractive features, such as almost negligible vapor pressure and high thermal and chemical stability. IL based extractive distillation is a potential alternative to the extractive distillation using a volatile organic solvent as an entrainer (Seiler et al., 2004, Lei et al., 2014b, Corderí et al., 2013).

To evaluate the potential of using ILs as non-volatile entrainers for the separation of the azeotropic mixtures by extractive distillation, a widely used process for extractive distillation using ILs as entertainers is employed, as shown in Figure 3. There the distillation column is used to separate the light key component, 1, from the heavy key component, 2, and the entrainer (IL); subsequently the IL is regenerated by combining a flash drum and an air-operated, atmospheric stripper.

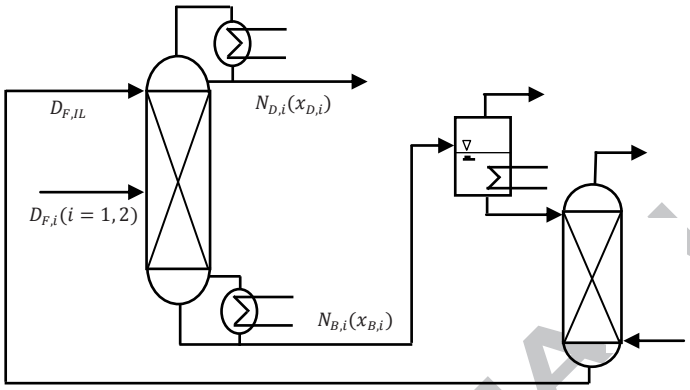

Figure 3: Ionic liquid-based extractive distillation process

Due to the large discrete IL molecular design space and the complex non-linear structure of the process design problem, shortcut models of processing units including a distillation column (Zhou et al., 2015), flash drum and stripper (Pereira et al., 2011) are introduced.

Distillation column

A shortcut model of distillation column expressed as ideal vapor, equilibrium stages, and constant relative volatilities throughout the column is considered. The pressure at the top and bottom of the column is set to 1 bar and 1.2 bar, respectively.

The molar flowrates ($D_{F,i}$,$N_{D,i}$, $N_{B,i}$) and compositions ($x_{D,i}$,$x_{B,i}$) of the distillate and bottom streams for component i are expressed as

$$N_{D,i} = D_{F,i} \cdot \vartheta_i \quad (25)$$

$$N_{B,i} = D_{F,i} - N_{D,i} \quad (26)$$

$$x_{D,i} = \frac{N_{D,i}}{\sum_{i \in COM} N_{D,i}} \quad (27)$$

$$x_{B,i} = \frac{N_{B,i}}{\sum_{i \in COM} N_{B,i}} \quad (28)$$

where ϑ_i represents the recovery of the key component i in the distillate. *COM* is the set of all component i involved in the specified separation process. Due to no IL assumed to be present in the vapor phase ($N_{D,IL} = 0$) and the IL is fed at the top of the column, the molar flowrate of IL throughout the column is equal to the feed of IL ($N_{F,IL}$).

For the same reason of the negligible vapor pressure exhibited by ILs, only light key component (component 1) and heavy key component (component 2) are assumed to be present in the vapor phase, and then the VLE can be expressed as

$$P = x_1\gamma_1 P_1^{sat} + x_2\gamma_2 P_2^{sat} \quad (29)$$

$$Py_i = x_i\gamma_i P_i^{sat} \quad i = 1,2 \quad (30)$$

where P_1^{sat} and P_1^{sat}, respectively, represent the saturated pressure of component 1 and 2. y_i are the vapor compositions for component $i(i = 1,2)$.

The Antoine equation is used to predict the saturated pressure, as shown in Eq.31

$$lnP_i^{sat} = A_i - \frac{B_i}{T+C_i} \quad i = 1,2 \quad (31)$$

Relative volatilities at the top ($\alpha_{1,2}^D$) and bottom ($\alpha_{1,2}^B$) of the column are represented as

$$\alpha_{1,2}^D = \frac{\gamma_1^D P_1^{sat,D}}{\gamma_2^D P_2^{sat,D}} \quad (32)$$

$$\alpha_{1,2}^B = \frac{\gamma_1^B P_1^{sat,B}}{\gamma_2^B P_2^{sat,B}} \quad (33)$$

where γ_1^D, γ_2^D are the activity coefficient of component 1 and component 2 at the top of the column while γ_1^B, γ_2^B are the activity coefficient of component 1 and component 2 at the bottom of the column, respectively. Similarly, $P_1^{sat,D}$, $P_2^{sat,D}$ are the saturated pressure of component 1 and component 2 at the top of the column while $P_1^{sat,B}$, $P_2^{sat,B}$ are the saturated pressure of component 1 and component 2 at the bottom of the column, respectively. Since the IL is fed at the top of the column and therefore the relative volatility calculation at the top, i.e. $\alpha_{1,2}^D$, in Eq.32 also includes the IL.

The average relative volatility of the component 1 and component 2 throughout the column is defined as

$$\alpha_{1,2} = \sqrt{\alpha_{1,2}^D \cdot \alpha_{1,2}^B} \quad (34)$$

In order to estimate the column size (N_t) and reflux ratio (R), the Westerberg method (Pereira et al., 2011) is employed in this work and the value of arbitrary weights φ_N and φ_R are set as 0.8

$$N_{lk} = 12.3/\left(\left(\alpha_{1,2} - 1\right)^{2/3} \cdot (1 - \vartheta_1)^{1/6}\right) \quad (35)$$

$$N_{hk} = 12.3/\left(\left(\alpha_{1,2} - 1\right)^{2/3} \cdot {\vartheta_2}^{1/6}\right) \quad (36)$$

$$R_{lk} = 1.38/\left(\left(\alpha_{1,2} - 1\right)^{0.9} \cdot (1 - \vartheta_1)^{0.1}\right) \quad (37)$$

$$R_{hk} = 1.38/\left(\left(\alpha_{1,2} - 1\right)^{0.9} \cdot {\vartheta_2}^{0.1}\right) \quad (38)$$

$$N_t = \varphi_N max\{N_{lk}, N_{hk}\} + (1 - \varphi_N) min\{N_{lk}, N_{hk}\} \quad (39)$$

$$R = \varphi_R max\{R_{lk}, R_{hk}\} + (1 - \varphi_R) min\{R_{lk}, R_{hk}\} \quad (40)$$

In Eqs.35-40, indices lk, hk represent the key component with low volatility and high volatility, respectively. For the ternary system containing IL, compound 1 is lk, compound 2 is hk and compound 3 is the IL. In this design method, the arbitrary weights were introduced to describe the non-ideality of the distillation.

Due to the extremely low vapor pressure exhibited by ILs as aforementioned, the saturation pressure for the ILs was assumed to be zero. As a result, no IL was assumed to be present in

the vapor phase. Therefore, the enthalpy of vaporization of the stream in the condenser and reboiler are calculated as molar weight sum of the enthalpies of vaporization of compound 1 and 2

$$\Delta H_{vap}^{B} = x_{B,i} \sum_{i=1,2} \Delta H_{vap}^{B,i} \quad 41$$

$$\Delta H_{vap}^{D} = x_{D,i} \sum_{i=1,2} \Delta H_{vap}^{D,i} \quad 42$$

where the temperature dependence of the enthalpy of vaporization can be obtained by Eq.43 proposed by Poling et al., (2011)

$$\Delta H_{vap}^{i} = \Delta H_{vap,298.15}^{i} \left(\frac{1-T/T_c^i}{1-298.15/T_c^i}\right)^{0.375} \qquad i = 1,2 \quad 43$$

As a result, the heat duties of the condenser and the reboiler is determined

$$Q_{reb} = \Delta H_{vap}^{B}(R+1) \sum_{i=1,2} N_{D,i} \quad 44$$

$$Q_{cond} = \Delta H_{vap}^{D}(R+1) \sum_{i=1,2} N_{D,i} \quad 45$$

Flash drum (Douglas, 1988)

The size of the flash drum can be determined by

$$V_{vessel} = 2F_{liquid} \epsilon V_{liquid} \quad 46$$

Where, F_{liquid} is the liquid molar flowrate ($mol.s^{-1}$) and V_{liquid} is the molar volume of liquid (m^3) and a residence time ϵ of 300 (s) is considered.

Stripper

The stripper is represented by a shortcut model containing several assumptions such as complete mixing, thermodynamic equilibrium and constant tray efficiency throughout the column.

The number of theoretical stages of the stripper for a given separation can be estimated as follows (Kohl and Nielsen, 1997)

$$N_e = \left((S/(S-1)) \ln(1-1/S)\, x_{IN,2}/x_{OUT,2} + 1/S\right) \quad 47$$

Where, $S = mG/L$ (G: molar flowrate of gas; L: molar flowrate of liquid) is the stripping factor, $x_{IN,2}$ = inlet concentration of compound 2, $x_{OUT,2}$ = outlet concentration of compound 2; $m = \gamma P^{sat}/P$ is the phase equilibrium constant.

An overall tray efficiency factor E_0 defined as Eq.48 is used to express the tray efficiency throughout the column

$$E_0 = N_e/N_a \quad 48$$

N_a is the actual number of trays, based on which the tray stack height h and the column height H can be determined

$$h = N_a TS \quad 49$$

$$H = 1.15 N_a TS \quad 50$$

Where, the tray spacing TS is set to 0.6096 m and the overall tray efficiency E_0 is assumed to be 0.2.

The column diameter of the stripper can be calculated as follows

$$D = 2\sqrt{\frac{A_t}{\pi}} \quad 51$$

$$A_t = 1.2A_n \quad 52$$

$$A_n = q_V/U_n \quad 53$$

$$U_n = 0.8U_{n,flood} \quad 54$$

Where, A_t and A_n represent the total cross section and the net area of the column (m^2), respectively. q_V is the volume flowrate of air ($m^3.s^{-1}$) fed at the bottom of the column, and the $U_{n,flood}$ is obtained using Eq.67 proposed by Perry et al. (1997)

$$U_{n,flood} = C_{sb,flood} \cdot \left(\frac{\sigma_L}{20}\right)^{0.2} \cdot \sqrt{\frac{\rho_L - \rho_V}{\rho_V}} \quad 55$$

In Eq.55, σ_L is the liquid surface tension (mNm^{-1}) that can be calculated by Eq.9; ρ_L, ρ_V are the densities of liquid and gas ($kg.m^{-3}$). $C_{sb,flood}$ is obtained from a correlation established by (Lygeros and Magoulas, 1986), and is expressed as a function of the tray spacing TS (inches) and a ratio of liquid to vapor kinetic energy through F_{LV}

$$C_{sb,flood} = 0.0105 + 8.127 \times 10^{-4}(25.4TS)^{0.755} e^{(-1.463F_{LV}^{0.842})} \quad 56$$

$$F_{LV} = \sqrt{\frac{\rho_L}{\rho_V}} \frac{q_L}{q_V} \quad 57$$

In Eq.57, q_L represents the volumetric liquid flowrate ($m^3.s^{-1}$). It can be calculated based on the information of liquid molar flowrate, density and molar weight.

3.2. Cost models

To evaluate the economic performance of the IL-based extractive distillation process, the annual cost of processing units including distillation column (AC_{dis}), flash drum (AC_{drum}), and stripper ($AC_{stripper}$) needs be calculated. Cost models used in (Zhou et al., 2015) and (Pereira et al., 2011) are adopted in this work. The total annual cost (TAC) of the separation process is applied as our performance objective in this integrated design method. In order to obtain a practical and applicable process design, the boundaries of some variables are introduced. For example, the boundary of the solvent flowrate ($D_{F,IL}$) is intended to be economically considered and an upper bound of the operating temperature in the flash drum (T_{drum}) is introduced to avoid decomposition of the IL. Similarly, considering the processing operations, reasonable constraints on some properties of IL (e.g. T_m, η) are included as well. The units of cost, utility and temperature are US \$/year, J and K, respectively, in the following calculation.

The capital investment of the distillation column (CI_{col}) contributed by the cost of trays and the cost of the column vessel

$$CI_{col} = \left((N_t/0.8) \times 500 + \left((N_t/0.8 - 1) \times 0.6 + 6\right) \times 2500\right)/3 \quad 58$$

The heat transfer areas of the heat exchanger (S_{heater}), condenser (S_{cond}) and reboiler (S_{reb}) can be calculated by

$$S_{heater} = Q_H/\left(\frac{T_F - T_0}{\ln((423 - T_0)/(423 - T_F))} \times 1420\right) \quad 59$$

$$S_{reb} = Q_{reb}/\left((493 - T_{bub}) \times 1420\right) \quad 60$$

$$S_{cond} = Q_{cond}/(567.8 \times 20/\ln((T_{dew} - 300)/(T_{dew} - 320))) \quad 61$$

where T_{bub} and T_{dew} are the bubble and dew temperatures at reboiler and condenser.

The capital cost of heat exchange units (CI_u) can be calculated by their corresponding base cost (BC_u), where u represents heat exchanger, reboiler and condenser.

$$BC_u = 300 \times (S_u/0.51)^{0.024} \quad 62$$

$$CI_u = BC_u \times 3.12 \times (1.83 + 1.35 - 1)/3 \quad 63$$

$$CI_{dis} = CI_{col} + \sum_u CI_u \quad 64$$

The utility cost of the heat exchanger (UC_{heater}), condenser (UC_{cond}), reboiler (UC_{reb}) and distillation column (UC_{dis}) are given by

$$UC_{cond} = 330 \times 24 \times 60 \times 60 \times Q_{cond} \cdot \tau_{CW}/(75.33 \times 20) \quad 65$$

$$UC_{heater} = 330 \times 24 \times 60 \times 60 \times Q_H \cdot \tau_{HS}/38012.4 \quad 66$$

$$UC_{reb} = 330 \times 24 \times 60 \times 60 \times Q_{cond} \cdot \tau_{HS}/33303.6 \quad 67$$

$$UC_{dis} = UC_{cond} + UC_{heater} + UC_{reb} \quad 68$$

$$AC_{dis} = CI_{dis} + UC_{dis} \quad 69$$

where the price of hot steam (τ_{HS}) and the price of cooling water (τ_{CW}) are set to 0.00012 (US $/mol) and 2.47E-7 (US $/mol), respectively.

The purchase cost of the flash drum, $CI_{drum}$is a function of the volume of the flash drum V_{drum} (m³) and the pressure factor, F_p determined by the pressure of flash drum, P_{drum} (MPa); The utility cost of the flash drum (UC_{drum}) depends on its heat duty (Q_{drum}) and τ_{HS}

$$AC_{drum} = CI_{drum} + UC_{drum} \quad 70$$

$$CI_{drum} = 4832.42 F_p V_{drum}^{0.6287} \quad 71$$

$$F_p = 0.057375 P_{drum}^2 + 0.05805 P_{drum} + 1.0136 \quad 72$$

$$UC_{drum} = 330 \times 24 \times 60 \times 60 \times Q_{drum} \cdot \tau_{HS}/33303.6 \quad 73$$

The annual cost of stripper is:

$$AC_{stripper} = CI_{shell} + CI_{trays} \quad 74$$

The cost of the shell (CI_{shell}) is calculated as:

$$CI_{shell} = 3185 F_p D^{1.066} H^{0.82} \quad 75$$

where D is the column diameter in m, H is the column height in m, and F_p is the pressure factor; the cost of the trays (CI_{trays}) is a function of the tray stack height h (m), the diameter D (m), and factor F_c (is set to 1 in this work):

$$CI_{trays} = 323.3 F_p D^{1.55} h F_c \quad 76$$

4. MINLP formulation and solution (application example)

The objective of this work is to simultaneously identify optimal IL and the corresponding separation process design corresponding to the best economic performance, subjecting to a list

of constraints involving molecular structure, IL properties, process model and operating conditions.

Problem details

The integrated IL and process design involving extractive distillation schemes can be formulated as an MINLP optimization problem summarized in Table 1:

Table 1: Integrated design (MINLP) problem formulation

Minimize:	TAC = AC_{dis} + AC_{drum} + $AC_{stripper}$
Variables:	Binary: vectors c_i $(i \epsilon C)$, a_j $(j \epsilon A)$, x_l $(1 \leq l \leq N)$ Integer: vectors n_{kl} , v_{kl} $(1 \leq l \leq N;\ k \epsilon S)$, v_i $(i \epsilon C)$ Continuous: temperature, flowrate, composition, equipment sizes….
s.t.	Variable boundaries: $0 < D_{F,IL} < 100$ (kmol/h), $T_{drum} < 500$ (K)
	IL structure constraints: Chemical feasibility: Eqs.18–22 Chemical complexity: Eqs.23–24
	IL property constraints: Physical property estimation: Eqs.1–11 Property boundary: $T_m < T_p - 5$ (K), $\eta < 0.05$ (Pa.s)
	Thermodynamic model: UNIFAC-IL: Eqs.A1-A12
	Process models: Distillation column: Eqs.25–45 Flash Drum: Eq.46 Stripper: Eqs.47-57
	Economic models: AC_{dis}: Eqs.58–69 AC_{drum}: Eqs.70–73 $AC_{stripper}$: Eqs.74–76

In this work, case studies including ethanol-water separation (Case 1) and acetone-methanol separation (Case 2) are performed to demonstrate the proposed methodology. For both cases, deterministic global optimization solver, LINDOGLOBAL, is used to solve the formulated MINLP problems in the modelling system GAMS 24.4.6 on an Intel(R) Xeon(R) E5-1620 3.70 GHz PC running Windows 10 system. The same optimization solution was observed for each case by using many initializations. Additionally, different well-known MINLP solvers (e.g. BARON, CONOPT) have been tried to solve the formulated problems but without success due to convergence problems. Table 2 gives information on the number of variables and constraints of the formulated MINLP problems and Table 3 provides the model statistics from GAMS solution for Case 1 and Case 2. Detailed results of the case studies are given in the following sections.

Table 2: Information of the formulated MINLP problems in terms of size of each vector of variables and constraints

Size of the vectors

	z	y		$g_p(z,y)$	$g_t(z,y)$	$g_m(y)$	Nonlinear constraints
		Binary	Integer				
Case 1	568	15	62	137	404	10	472
Case 2	569	13	62	138	404	10	472

Table 3: Model statistics from GAMS solution for Case 1 and Case 2

	Number of continuous variables	Number of binary variables	Number of equations	Number of constraints	Number of iterations	CPU time (s)
Case 1	568	15	551	551	938401	349
Case 2	569	13	552	552	17811	64

Property model parameters

For these two case studies, group volume (R_k) and surface area (Q_k) parameters, and interaction parameters (a_{nm}, a_{mn}) between IL groups and conventional groups are taken from the original UNIFAC model (Wittig et al., 2003, Roughton et al., 2012); Roughton et al., 2012). In their work, the R_k and Q_k are estimated based on the rules of Bondi (Bondi, 1964) while the a_{nm} and a_{mn} are obtained based on a wide range of available experimental data on activity coefficients of various solutes at infinite dilution in ILs by minimizing the objective function (Eq.89)

$$OF = \sum_i^N \left| \frac{\gamma_i^{\infty,exp} - \gamma_i^{\infty,calc}}{\gamma_i^{\infty,exp}} \right| \quad (89)$$

where $\gamma_i^{\infty,exp}$ and $\gamma_i^{\infty,calc}$ represent the experimental and calculated infinite dilution activity coefficients of the solutes (i) in ILs, respectively. N is the total number of infinite dilution activity coefficients (γ^{∞}) data points. Meanwhile, comparisons between the UNIFAC-IL predictions and experimental ternary VLE data of several binary azeotropes (ethanol–water, acetone–methanol, ethyl acetate–ethanol, 1-propanol–water and 2-propanol–water) with some ILs have been presented to validate the performance of the UNIFAC-IL model (Roughton et al., 2012).

In order to compare economic performance of the whole extractive distillation process using the optimal IL identified in this work and previous works, fixed process parameters including column operating pressure, composition of feed and distillate used by (Roughton et al., 2012) were applied. Well-studied groups containing 2 substituents, 2 cations and 7 anions were selected as molecular building blocks for the IL design, as shown in Table 4.

Table 4: Molecular building blocks selected for IL design

Type	Groups	Type	Groups
Substituents	CH_3	Anions	$[Tf_2N]^-$
	CH_2		$[BF_4]^-$
Cation cores	$[Im]^+$		$[PF_6]^-$
	$[Py]^+$		$[CF_3SO_3]^-$

	$[CF_3COO]^{-*}$
	$[DMP]^{-}$
	$[SCN]^{-*}$

*NB: Groups only used in the case study of ethanol-water separation

4.1. Ethanol –water separation

The task of the ethanol-water separation process can be expressed as a 200 $kmol.h^{-1}$ liquid mixture consisting of 70 mol% ethanol and 30 mol% water, to be separated by extractive distillation that the ethanol composition of distillate (140 $kmol.h^{-1}$) amounts to 99.8 mol%. Fixed process parameters (i.e., column operating pressure, flowrate and composition of feed and distillate….) are given in Table 5.

Table 5: Fixed parameters of the ethanol-water separation process

Fixed parameters	Value
Distillation column	
Pressure at the top	1 atm
Pressure at the bottom	1.2 atm
Feed rate and composition	200 kmol/h, (0.7 C_2H_5OH, 0.3 H_2O)
Distillate flowrate	140 kmol/h
Molar composition of distillate	0.998 C_2H_5OH
Flash drum	
Operating pressure	0.1 atm
Stripper	
Air temperature	298.15 K
Molar composition of IL at the bottom	0.999

For the case study of ethanol-water separation process, free variables such as: (1) IL structure, (2) IL flowrate, (3) reflux ratio, (4) size of the processing units (e.g. number of column trays, volume of flash drum), (5) temperature of the flash drum, and (6) air flow in the stripping column should be optimized to achieve the best economic performance of the overall extractive distillation process. A set of constraints of these variables are introduced to make sure the designed ILs and the process operations are feasible for industrial applications. Optimization results, including the best IL molecular structure and the corresponding optimal distillation column design variables are simultaneously obtained by solving the formulated MINLP problem (given in Table 6). Meanwhile, two nonlinear programming (NLP) problems of reference design are also formulated and solved as comparisons.

In this case, 1-methylpyridinium hexafluorophosphate ($[mPy]^+[PF_6]^-$) is found to be the best IL as a solvent with an economically attractive TAC of 719 733 US $/year. For the same ethanol-water separation task, (Seiler et al., 2004) used experimentally selected IL, 1-ethyl-3-methylimidazolium tetrafluoroborate ($[emIm]^+[BF_4]^-$) as an entrainer and (Roughton et al., 2012) determined 1, 3-dimethylimidazolium dimethylphosphate ($[mmIm]^+[DMP]^-$) as an entrainer based on the CAMD method using the Hildebrand solubility parameter of azeotropic mixtures as a target. For comparing the economic performance of this ethanol-water separation process using ILs identified through different methods, integrated these two fixed ILs and the same process models used in this work, optimization results (see Table 6) give TAC values of 916 144 US$, and 1 073 665 US$, respectively, also achieved by solving their corresponding NLP problems.

As shown in Table 6, AC_{drum} contributes major cost to TAC when using all three ILs as solvents, indicating that the economic performance of this separation process mainly depends on the relative volatility of the components to be separated, which indirectly reflects the importance of their activity coefficients in the IL containing system. In this case, all contributions (i.e. AC_{drum}, AC_{drum}, $AC_{stripper}$) of the TAC using $[mPy]^+[PF_6]^-$ are the lowest compared to the other two referenced ILs. Despite the fact that both the experimentally selected $[emIm]^+[BF_4]^-$ and the CAMD-based designed $[mmIm]^+[DMP]^-$ have better performance of the minimum concentration to break azeotrope (ethanol-water), nevertheless, $[mPy]^+[PF_6]^-$ identified in this work, is considered the best one with the highest economic performance (TAC). This result highlights the necessity of investigating trade-offs among different solvent properties to obtain the best overall process performance. It also indicates that the proposed integrated IL and process design method allow the identification of the best IL and the corresponding optimal process conditions which would lead to a considerable decrease in TAC. The structures of ILs involved in this case study are given in Figure 4.

Table 6: Optimization results of the proposed integrated design and the reference design problems for the ethanol-water separation process

Optimization Variable	This work	Solvent 1 (Seiler et al., 2004)	Solvent2 (Roughton et al., 2012)
Ionic liquid			
Molecule	$[mPy]^+[PF_6]^-$	$[emIm]^+[BF_4]^-$	$[mmIm]^+[DMP]^-$
Cation	$[Py]^+$	$[Im]^+$	$[Im]^+$
Anion	$[PF_6]^-$	$[BF_4]^-$	$[DMP]^-$
Valence of the cation base	1	2	2
Number of CH_3 in side 1	1	1	1
Number of CH_3 in side 3	0	1	1
Number of CH_2 in side 3	0	1	0
Flowrate (kmol/h)	67.0	73.1	65.4
Distillation column			
Number of trays N_t	9	13	14
Reflux ratio R	0.442	0.714	0.789
AC_{column} (US $/year)	431 008	525 801	550 459
Flash drum			
T_{drum} (K)	444.8	446.0	471.3
AC_{drum} (US $/year)	142 682	150 951	216 058
Stripper			
Number of stages N_a	17	18	22
Air flowrate q_V (kmol/h)	463.6	521.0	559.5
$AC_{stripper}$ (US $/year)	146 043	239 392	307 158
TAC (US $/year)	719 733	916 144	1 073 665

4.2. Acetone-methanol separation

The separation task of acetone-water can be represented as follows: 200 $kmol.h^{-1}$ liquid mixture consisting of 50 mol% acetone and 50 mol% methanol, to be separated by extractive distillation, such that the acetone purity of the distillate (100 $kmol.h^{-1}$) amounts to 99.5 mol%. Fixed process parameters (i.e., column operating pressure, flowrate and composition of feed and distillate….) are given in Table 7.

As well as the separation of ethanol-water, to determine the minimum TAC of the overall extractive distillation process, the following variables: (1) IL structure, (2) IL flowrate, (3) reflux ratio, (4) size of the processing units, (5) temperature of the flash drum, and (6) air flow in the stripping column should be optimized. The best IL molecular structure and the optimal flowsheet configurations are simultaneously identified by solving the formulated MINLP problem. A selected optimisation results of the integrated IL and process design, and two reference design problems for the acetone-methanol separation are given in Table 8.

In this case, 1, 2, 3-trimethylimidazolium dimethylphosphate ($[C_1mmIm]^+[DMP]^-$) is found to be the best IL as a solvent with a minimum TAC of 775 216 US $/year. Two solvents, 3-methyl-1-octylpyridinium trifluoromethanesulfonate ($[omPy]^+[CF_3SO_3]^-$) and 1-ethyl-3-methylimidazolium trifluoromethanesulfonate ($[emIm]^+[CF_3SO_3]^-$) investigated by (Roughton et al., 2012) are considered for comparison. In their work, $[omPy]^+[CF_3SO_3]^-$ was experimentally selected while $[emIm]^+[CF_3SO_3]^-$ was identified based on the CAMD method using the Hildebrand solubility parameter of the azeotropic mixture, as a target. For using these two fixed ILs and the same process and economic models as integrated design cases, optimization results are also obtained by solving their corresponding NLP problems in this work. As shown in Table 8, the total costs of the optimization process using these two ILs as solvents are 959 870 US $/year and 1 019 379 US $/year, respectively.

Table 7: Fixed parameters of the acetone-methanol separation process

Fixed parameters	Value
Distillation column	
Pressure at the top	1 atm
Pressure at the bottom	1.2 atm
Feed rate and composition	200 kmol/h, (0.5 $(CH_3)_2CO$, 0.5 CH_3OH)
Distillate flowrate	100 kmol/h
Molar composition of distillate	0.995 $(CH_3)_2CO$
Flash drum	
Operating pressure	0.1 atm
Stripper	
Air temperature	298.15 K
Molar composition of IL at the bottom	0.999

Table 8: Optimization results of the proposed integrated design and the reference design problems for the acetone-methanol separation process

Optimization Variable	This work	Solvent1 (Roughton et al., 2012)	Solvent2 (Roughton et al., 2012)
Ionic liquid			
Molecule	$[C_1mmIm]^+$ $[DMP]^-$	$[emIm]^+$ $[CF_3SO_3]^-$	$[omPy]^+$ $[CF_3SO_3]^-$
Cation	$[Im]^+$	$[Im]^+$	$[Py]^+$
Anion	$[DMP]^-$	$[CF_3SO_3]^-$	$[CF_3SO_3]^-$
Valence of the cation base	3	2	2
Number of CH_3 in side 1	1	1	1
Number of CH_3 in side 2	1	0	0
Number of CH_3 in side 3	1	1	1

Number of CH_2 in side 3	0	1	7
Flowrate (kmol/h)	56.1	38.1	56.3
Distillation column			
Number of trays N_t	20	32	27
Reflux ratio R	1.309	2.474	1.999
AC_{column} (US $/year)	592 620	884 003	768 664
Flash drum			
T_{drum} (K)	366.8	364.7	369.0
AC_{drum} (US $/year)	67 670	64 590	84 154
Stripper			
Number of stages N_a	22	21	22
Air flowrate q_V (kmol/h)	366.8	177.6	298.6
$AC_{stripper}$ (US $/year)	114 927	70 786	107 052
TAC (US $/year)	775 216	1 019 379	959 870

Same as the separation of ethanol-water mixture, AC_{drum} also provides major contribution to the TAC in this case (see Table 8). The results reinforce the effect of the relative volatility of components to be separated on the economic performance of the separation process. Since the relative volatility of the components to be separated depends on their activity coefficients in the IL containing system, therefore, the thermodynamic property of IL plays the main role in the separation process. Unlike the first case, contributions of AC_{drum} and $AC_{stripper}$ using referenced IL, $[emIm]^+[CF_3SO_3]^-$, are the lowest among all three IL solvents in this case, this is mainly because of its lowest flowrate. However, compared to the two reference cases, the integrated design method proposed in the present work is capable of simultaneously identifying the optimal IL and the corresponding optimal process configurations which can significantly improve the overall economic performance (lower TAC). Although the separation process using $[C_1mmIm]^+[DMP]^-$ as an entrainer has the best economic performance, both the CAMD-based determined $[omPy]^+[CF_3SO_3]^-$ and the experimentally selected $[emIm]^+[CF_3SO_3]^-$ can break this azeotrope at a lower concentration, especially the process using $[emIm]^+[CF_3SO_3]^-$ has the lowest AC_{drum}, $AC_{stripper}$ and the flowrate of IL, which indicates the importance of investigating trade-offs among different IL properties for process design. The structures of ILs involved in this case study are also given in Figure 4.

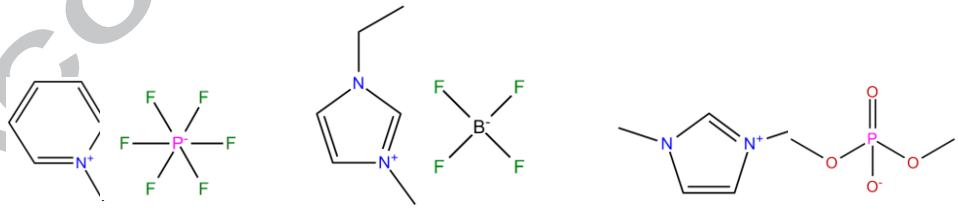

(a) (b) (c)

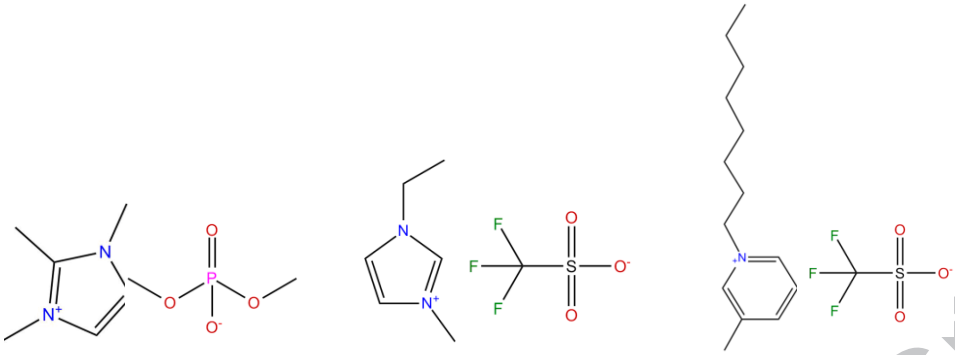

(d) (e) (f)

Figure 4. The structure of six ionic liquids involved in case studies:
(a) $[mPy]^+[PF_6]^-$, (b) $[emIm]^+[BF_4]^-$, (c) $[mmIm]^+[DMP]^-$, (d) $[C_1mmIm]^+[DMP]^-$
(e): $[emIm]^+[CF_3SO_3]^-$, (f) $[omPy]^+[CF_3SO_3]^-$

5. Conclusions

A systematic method combining GC-based property models, UNIFAC-IL models, CAMD and process design, representing CAILD, to simultaneously determine the optimal IL as a separating agent and the corresponding optimal process design has been developed. In this method, all groups (i.e. cations, anion, substituents) contained in IL molecular are treated separately and the cost of IL regeneration is also included. Case studies involving separation of azeotropic mixtures such as ethanol-water and acetone-methanol have been presented to evaluate the performance of this integrated design method. A set of constraints on rules of combination and properties of ILs are introduced to ensure the designed ILs are chemically feasible. The IL molecular structure and the process variables are optimized simultaneously by the formulation and solution of MINLP problems using economic performance (TAC) as the objective function. Comparisons between the achieved economic performance of the whole extractive distillation process using optimal IL identified in this work and previous work(s) highlights the importance of investigating trade-offs among different properties of ILs to obtain the best overall process performance, and also verify the proposed integrated design method. The optimization results of the MINLP problems are further evaluated by detailed process analysis. We should note that the applicability and reliability of the calculation results would be improved if experimental validation is available.

Because of the limited group parameters for IL containing systems, only well-studied groups of ILs are considered as building blocks in this work. However, the developed methodology can easily be extended to other ILs, once their group parameters are available. We are currently extending the model library for IL properties as well as a wide range of IL-based separation processes.

Acknowledgements

This research work was supported by the China Scholarship Council (No. 201708440264) and the Technical University of Denmark. The authors would like to thank PhD student Nipun Garg from the Technical University of Denmark. His suggestions and comments were much appreciated.

References

BABI, D. K., HOLTBRUEGGE, J., LUTZE, P., G RAK, A., WOODLEY, J. M. & GANI, R. 2015. Sustainable process synthesis–intensification. *Computers & Chemical Engineering,* 81**,** 218-244.

BARTON, P. 2000. Solvent recovery opportunities in the pharmaceutical industry. *Current opinion in drug discovery & development,* 3**,** 707-713.

BENEDICT, M. & RUBIN, L. C. 1945. Extractive and azeotropic distillation. *Theoretical Aspects. Trans. Am. Inst. Chem. Eng,* 41**,** 353-370.

BONDI, A. 1964. van der Waals volumes and radii. *The Journal of physical chemistry,* 68**,** 441-451.

BURGER, J., PAPAIOANNOU, V., GOPINATH, S., JACKSON, G., GALINDO, A. & ADJIMAN, C. S. 2015. A hierarchical method to integrated solvent and process design of physical CO2 absorption using the SAFT - γ Mie approach. *AIChE Journal,* 61**,** 3249-3269.

CHAO, H., SONG, Z., CHENG, H., CHEN, L. & QI, Z. 2017. Computer-aided design and process evaluation of ionic liquids for n-hexane-methylcyclopentane extractive distillation. *Separation and Purification Technology*.

CHEN, Y., KONTOGEORGIS, G. M. & WOODLEY, J.M. 2019. Group Contribution Based Estimation Method for Properties of Ionic Liquids. *Industrial & Engineering Chemistry Research,* 58, 4277-4292.

CHEN, Y., WOODLEY, J.M., KONTOGEORGIS, G.M. & GANI, R. 2018. Integrated Ionic Liquid and Process Design involving Hybrid Separation Schemes. *Computer Aided Chemical Engineering,* 44, 1045-1050.

CHONG, F. K., ELJACK, F. T., ATILHAN, M., FOO, D. C. & CHEMMANGATTUVALAPPIL, N. G. 2016. A systematic visual methodology to design ionic liquids and ionic liquid mixtures: Green solvent alternative for carbon capture. *Computers & Chemical Engineering,* 91**,** 219-232.

CHONG, F. K., FOO, D. C., ELJACK, F. T., ATILHAN, M. & CHEMMANGATTUVALAPPIL, N. G. 2015. Ionic liquid design for enhanced carbon dioxide capture by computer-aided molecular design approach. *Clean Technologies and Environmental Policy,* 17**,** 1301-1312.

CORDER , S., GONZ LEZ, B., CALVAR, N. & G MEZ, E. 2013. Ionic liquids as solvents to separate the azeotropic mixture hexane/ethanol. *Fluid Phase Equilibria,* 337**,** 11-17.

DAI, C., LEI, Z., WANG, W., XIAO, L. & CHEN, B. 2013. Group contribution lattice fluid equation of state for CO2–ionic liquid systems: an experimental and modeling study. *AIChE Journal,* 59**,** 4399-4412.

DIEDENHOFEN, M., ECKERT, F. & KLAMT, A. 2003. Prediction of infinite dilution activity coefficients of organic compounds in ionic liquids using COSMO-RS. *Journal of Chemical & Engineering Data,* 48**,** 475-479.

DOUGLAS, J. M. 1988. *Conceptual design of chemical processes*, McGraw-Hill New York.

FANG, J., ZHAO, R., SU, W., LI, C., LIU, J. & LI, B. 2016. A molecular design method based on the COSMO - SAC model for solvent selection in ionic liquid extractive distillation. *AIChE Journal,* 62**,** 2853-2869.

GANI, R., NIELSEN, B. & FREDENSLUND, A. 1991. A group contribution approach to computer - aided molecular design. *AIChE Journal,* 37**,** 1318-1332.

GARDAS, R. L. & COUTINHO, J. A. 2009. Group contribution methods for the prediction of thermophysical and transport properties of ionic liquids. *AIChE Journal,* 55**,** 1274-1290.

GMEHLING, J. & RASMUSSEN, P. 1977. *Vapor-liquid equilibria using UNIFAC: a group-contribution method*, Elsevier.

GMEHLING, J., RASMUSSEN, P. & FREDENSLUND, A. 1982. Vapor-liquid equilibriums by UNIFAC group contribution. Revision and extension. 2. *Industrial & Engineering Chemistry Process Design and Development,* 21**,** 118-127.

HARPER, P. M., GANI, R., KOLAR, P. & ISHIKAWA, T. 1999. Computer-aided molecular design with combined molecular modeling and group contribution. *Fluid Phase Equilibria,* 158**,** 337-347.

HECTOR, T. & GMEHLING, J. 2014. Present status of the modified UNIFAC model for the prediction of phase equilibria and excess enthalpies for systems with ionic liquids. *Fluid Phase Equilibria,* 371**,** 82-92.

HOLBREY, J. & SEDDON, K. 1999. Ionic liquids. *Clean Technologies and Environmental Policy,* 1**,** 223-236.

HUANG, Y., DONG, H., ZHANG, X., LI, C. & ZHANG, S. 2013. A new fragment contribution - corresponding states method for physicochemical properties prediction of ionic liquids. *AIChE Journal,* 59**,** 1348-1359.

JACQUEMIN, J., GE, R., NANCARROW, P., ROONEY, D. W., COSTA GOMES, M. F., P DUA, A. A. & HARDACRE, C. 2008a. Prediction of ionic liquid properties. I. Volumetric properties as a function of temperature at 0.1 MPa. *Journal of Chemical & Engineering Data,* 53**,** 716-726.

JACQUEMIN, J., NANCARROW, P., ROONEY, D. W., COSTA GOMES, M. F., HUSSON, P., MAJER, V., P DUA, A. A. & HARDACRE, C. 2008b. Prediction of ionic liquid properties. II. Volumetric properties as a function of temperature and pressure. *Journal of Chemical & Engineering Data,* 53**,** 2133-2143.

KARUNANITHI, A. & MEHRKESH, A. 2013. *Computer-Aided Design of Tailor-Made Ionic Liquids*.

KATO, R. & GMEHLING, J. 2005. Systems with ionic liquids: Measurement of VLE and $\gamma \infty$ data and prediction of their thermodynamic behavior using original UNIFAC, mod. UNIFAC (Do) and COSMO-RS (Ol). *The Journal of Chemical Thermodynamics,* 37**,** 603-619.

KLAMT, A. 1995. Conductor-like screening model for real solvents: a new approach to the quantitative calculation of solvation phenomena. *The Journal of Physical Chemistry,* 99**,** 2224-2235.

KLAMT, A. & ECKERT, F. 2000. COSMO-RS: a novel and efficient method for the a priori prediction of thermophysical data of liquids. *Fluid Phase Equilibria,* 172**,** 43-72.

KLAMT, A., JONAS, V., B RGER, T. & LOHRENZ, J. C. 1998. Refinement and parametrization of COSMO-RS. *The Journal of Physical Chemistry A,* 102**,** 5074-5085.

KOHL, A. L. & NIELSEN, R. 1997. *Gas purification*, Elsevier.

LAZZ S, J. A. 2009. ρ–T–P prediction for ionic liquids using neural networks. *Journal of the Taiwan Institute of Chemical Engineers,* 40**,** 213-232.

LEI, Z., CHEN, B. & LI, C. 2007. COSMO-RS modeling on the extraction of stimulant drugs from urine sample by the double actions of supercritical carbon dioxide and ionic liquid. *Chemical engineering science,* 62**,** 3940-3950.

LEI, Z., DAI, C. & CHEN, B. 2013. Gas solubility in ionic liquids. *Chemical reviews,* 114**,** 1289-1326.

LEI, Z., DAI, C., LIU, X., XIAO, L. & CHEN, B. 2012a. Extension of the UNIFAC model for ionic liquids. *Industrial & Engineering Chemistry Research,* 51**,** 12135-12144.

LEI, Z., DAI, C., WANG, W. & CHEN, B. 2014a. UNIFAC model for ionic liquid ‐ CO2 systems. *AIChE Journal,* 60**,** 716-729.

LEI, Z., DAI, C., ZHU, J. & CHEN, B. 2014b. Extractive distillation with ionic liquids: a review. *AIChE Journal,* 60**,** 3312-3329.

LEI, Z., XIAO, L., DAI, C. & CHEN, B. 2012b. Group contribution lattice fluid equation of state (GCLF EOS) for ionic liquids. *Chemical engineering science,* 75**,** 1-13.

LEI, Z., ZHANG, J., LI, Q. & CHEN, B. 2009. UNIFAC model for ionic liquids. *Industrial & Engineering Chemistry Research,* 48**,** 2697-2704.

LIN, S.-T., CHANG, J., WANG, S., GODDARD, W. A. & SANDLER, S. I. 2004. Prediction of vapor pressures and enthalpies of vaporization using a COSMO solvation model. *The Journal of Physical Chemistry A,* 108**,** 7429-7439.

LIN, S.-T. & SANDLER, S. I. 2002. A priori phase equilibrium prediction from a segment contribution solvation model. *Industrial & engineering chemistry research,* 41**,** 899-913.

LUTZE, P., GANI, R. & WOODLEY, J. M. 2010. Process intensification: a perspective on process synthesis. *Chemical Engineering and Processing: Process Intensification,* 49**,** 547-558.

LYGEROS, A. & MAGOULAS, K. 1986. Column flooding and entrainment. *Hydrocarbon processing,* 65**,** 43-44.

MORTAZAVI ‐ MANESH, S., SATYRO, M. A. & MARRIOTT, R. A. 2013. Screening ionic liquids as candidates for separation of acid gases: solubility of hydrogen sulfide, methane, and ethane. *AIChE Journal,* 59**,** 2993-3005.

MOUSAZADEH, M. & FARAMARZI, E. 2011. Calculation of surface tension of metals using density gradient theory and PC-SAFT equation of state. *Fluid Phase Equilibria,* 301**,** 13-17.

PALOMAR, J., GONZALEZ-MIQUEL, M., POLO, A. & RODRIGUEZ, F. 2011. Understanding the physical absorption of CO2 in ionic liquids using the COSMO-RS method. *Industrial & Engineering Chemistry Research,* 50**,** 3452-3463.

PEREIRA, F. E., KESKES, E., GALINDO, A., JACKSON, G. & ADJIMAN, C. S. 2011. Integrated solvent and process design using a SAFT-VR thermodynamic description: high-pressure separation of carbon dioxide and methane. *Computers & Chemical Engineering,* 35**,** 474-491.

PEREIRO, A. B. & RODR GUEZ, A. 2010. An ionic liquid proposed as solvent in aromatic hydrocarbon separation by liquid extraction. *AIChE journal,* 56**,** 381-386.

PETKOVIC, M., SEDDON, K. R., REBELO, L. P. N. & PEREIRA, C. S. 2011. Ionic liquids: a pathway to environmental acceptability. *Chemical Society Reviews,* 40**,** 1383-1403.

PLECHKOVA, N. V. & SEDDON, K. R. 2008. Applications of ionic liquids in the chemical industry. *Chemical Society Reviews,* 37**,** 123-150.

ROGERS, R. D. & SEDDON, K. R. 2003. Ionic liquids--solvents of the future? *Science,* 302**,** 792-793.

ROUGHTON, B. C., CHRISTIAN, B., WHITE, J., CAMARDA, K. V. & GANI, R. 2012. Simultaneous design of ionic liquid entrainers and energy efficient azeotropic separation processes. *Computers & Chemical Engineering,* 42**,** 248-262.

SANTIAGO, R. S., SANTOS, G. R. & AZNAR, M. 2009. UNIQUAC correlation of liquid–liquid equilibrium in systems involving ionic liquids: The DFT–PCM approach. *Fluid Phase Equilibria*, 278**,** 54-61.

SEILER, M., JORK, C., KAVARNOU, A., ARLT, W. & HIRSCH, R. 2004. Separation of azeotropic mixtures using hyperbranched polymers or ionic liquids. *AIChE Journal*, 50**,** 2439-2454.

SHAMSURI, A. A. 2011. Ionic liquids: preparations and limitations. *Makara Journal of Science*.

SHOLL, D. S. & LIVELY, R. P. 2016. Seven chemical separations: to change the world: purifying mixtures without using heat would lower global energy use, emissions and pollution--and open up new routes to resources. *Nature*, 532**,** 435-438.

SIMONI, L. D., CHAPEAUX, A., BRENNECKE, J. F. & STADTHERR, M. A. 2010. Extraction of biofuels and biofeedstocks from aqueous solutions using ionic liquids. *Computers & chemical engineering*, 34**,** 1406-1412.

SIMONI, L. D., LIN, Y., BRENNECKE, J. F. & STADTHERR, M. A. 2008. Modeling liquid− liquid equilibrium of ionic liquid systems with NRTL, electrolyte-NRTL, and UNIQUAC. *Industrial & Engineering Chemistry Research*, 47**,** 256-272.

SONG, Z., ZHANG, C., QI, Z., ZHOU, T. & SUNDMACHER, K. 2018. Computer‐aided design of ionic liquids as solvents for extractive desulfurization. *AIChE Journal*.

TIEGS, D., RASMUSSEN, P., GMEHLING, J. & FREDENSLUND, A. 1987. Vapor-liquid equilibria by UNIFAC group contribution. 4. Revision and extension. *Industrial & engineering chemistry research*, 26**,** 159-161.

VALENCIA-MARQUEZ, D., FLORES-TLACUAHUAC, A. & VASQUEZ-MEDRANO, R. 2011. Simultaneous optimal design of an extractive column and ionic liquid for the separation of bioethanol–water mixtures. *Industrial & Engineering Chemistry Research*, 51**,** 5866-5880.

VOORADI, R., BERTRAN, M.-O., FRAUZEM, R., ANNE, S. B. & GANI, R. 2017. Sustainable chemical processing and energy-carbon dioxide management: review of challenges and opportunities. *Chemical Engineering Research and Design*.

WELTON, T. 1999. Room-temperature ionic liquids. Solvents for synthesis and catalysis. *Chemical reviews*, 99**,** 2071-2084.

WITTIG, R., LOHMANN, J. & GMEHLING, J. 2003. Vapor− liquid equilibria by UNIFAC group contribution. 6. Revision and extension. *Industrial & engineering chemistry research*, 42**,** 183-188.

WOODLEY, J. M. 2017. Bioprocess intensification for the effective production of chemical products. *Computers & Chemical Engineering*.

WOODLEY, J. M., BISSCHOPS, M., STRAATHOF, A. J. & OTTENS, M. 2008. Future directions for in‐situ product removal (ISPR). *Journal of chemical technology and biotechnology*, 83**,** 121-123.

ZHAO, Y., GANI, R., AFZAL, R. M., ZHANG, X. & ZHANG, S. 2017. Ionic liquids for absorption and separation of gases: An extensive database and a systematic screening method. *AIChE Journal*, 63**,** 1353-1367.

ZHOU, T., MCBRIDE, K., ZHANG, X., QI, Z. & SUNDMACHER, K. 2015. Integrated solvent and process design exemplified for a Diels–Alder reaction. *AIChE Journal*, 61**,** 147-158.

Appendix A. UNIFAC

In the UNIFAC model, the activity coefficient of group i, γ_i, can be obtained by Eq.A1.

$$ln\,\gamma_i = ln\,\gamma_i{}^{C} + ln\,\gamma_i{}^{R} \quad \text{A1}$$

where the combinatorial part, $\gamma_i{}^{c}$, and the residual part, $\gamma_i{}^{R}$, can be calculated by Eqs.A2-A6 and Eqs.A7-A12, respectively.

$$ln\,\gamma_i{}^{c} = 1 - V_i + ln\,V_i - 5q_i(1 - \frac{V_i}{F_i} + ln(\frac{V_i}{F_i})) \quad \text{A2}$$

$$F_i = \frac{q_i}{\sum_j q_j x_j} \quad \text{A3}$$

$$V_i = \frac{r_i}{\sum_j r_j x_j} \quad \text{A4}$$

$$q_i = \sum_k v_k{}^{(i)} Q_k \quad \text{A5}$$

$$r_i = \sum_k v_k^{(i)} R_k \quad \text{A6}$$

where F_i and V_i are auxiliary properties for component i; the pure component parameters q_i and r_i, respectively, are relative molecular surface areas and molecular van der Waals volumes, which are calculated as the sum of the group area Q_k and group volume parameters R_k, respectively. $v_k^{(i)}$ denotes the number of groups of type k in molecule i.

$$ln\,\gamma_i^R = \sum_k v_k^{(i)} (ln\,\Gamma_k - ln\,\Gamma_k^{(i)}) \quad \text{A7}$$

$$ln\,\Gamma_k = Q_k (1 - ln(\sum_m \theta_m \psi_{mk}) - \sum_m \frac{\theta_m \psi_{km}}{\sum_n \theta_n \psi_{nm}} \quad \text{A8}$$

$$\theta_m = \frac{Q_m X_m}{\sum_n Q_n X_n} \quad \text{A9}$$

$$X_m = \frac{\sum_i v_m^{(i)} x_i}{\sum_i \sum_k v_k^{(i)} x_i} \quad \text{A10}$$

$$\psi_{nm} = exp[-(\alpha_{nm}/T)] \quad \text{A11}$$

$$\psi_{mn} = exp[-(\alpha_{mn}/T)] \quad \text{A12}$$

where Γ_k and $\Gamma_k^{(i)}$ represent the residual activity coefficient of group k and the residual activity coefficient of group k in pure component i, respectively; θ_m is the fraction of group m in a mixture of the liquid phase and X_m/X_n is the fraction of group m or n in the mixture; ψ_{nm} and $\psi_{mn}$are the group interaction parameters which can be calculated through Eq.A11 and A12 based on the value of UNIFAC group interaction parameters between group m and n, α_{nm} and α_{mn}.

Highlights

- A systematic method combining GC-based property models, UNIFAC-IL models, CAMD and process design is developed.
- The method is capable of simultaneously identifying the optimal IL and corresponding optimal process configurations by solving optimization-based integrated design problems.
- Considerable improvement in process economics is achieved with this method.